arXiv:1603.02081v1 [cond-mat.soft] 7 Mar 2016

Ordered Crumpled States in Twisted Ribbons

Julien Chopin* and Romildo T. D. Filho
Civil Engineering Department, COPPE, Universidade Federal do Rio de Janeiro, 21941-972, Rio de Janeiro RJ, Brazil

Elastic ribbons have emerged as a model system to explore the post-buckling regime of thin sheet including wrinkling and crumpling. Here, we investigate experimentally and theoretically the torsional and tensile response of a ribbon submitted to a twist under fixed longitudinal tension and clamped boundary conditions. Upon twisting, the shape of the ribbon is first a helicoid, then longitudinal wrinkles develop above a twist angle threshold and transform into flat triangular facets akin to an ordered crumpled state. In the pre-buckling regime, the measured torque and contraction show a nonlinear dependence with the twist angle which can be fully understood solving the Föppl-van Kármán equations. The post-buckling behavior is found to exhibit two regimes depending on the imposed tension T. In a high T regime, the contraction and torque are found to be in quantitative agreement with predictions obtained by a Far from Threshold (FT) approach. In a low T crumpled regime, the experimental data are best described using the concept of asymptotic isometry recently introduced when both tension and thickness are small.

Introduction

Ribbons, strips, belts are used in a wide range of industrial applications from sheet production to connectors in soft electronics [1], structural fibers [2] and graphene nanoribbons [3]. Ribbon geometry can also be found in Nature in a wide range of lengthscales from plant leaves, to beta sheets in proteins. In a recent study, the unique nature of the mechanics of ribbons was demonstrated using ribbons that are stretched and twisted [4, 5] yielding shapes with wrinkles, loops and ridges. In particular, at relatively small tension, triangular faceted helicoid corresponding to an ordered crumpled phase has been observed. Other model systems such as blisters [6], thin films on drop [7] and growing thin films [8] also exhibit a crumpled phase which remains poorly understood.

In this paper, we explore the route towards energy localization and characterized experimentally the mechanical behavior of a twisted ribbon in its crumpled phase measuring contraction and torque response. No experimental characterization of the energy stored in a crumpled ribbon has been reported so far which would give further insight of the crumpling transition and complement geometrical characterizations.

Modeling ribbons is a challenging task due to large deformations and finite rotations along with strong non linearities coupling strain and curvature [9]. A first approach, initiated by Sadowsky [10] and, later extended by Wunderlich [11], assume infinitely thin, strainless ribbons which greatly simplifies the problem as the ribbon surface is now developable allowing a reduction of dimensionality from 2D to 1D. A set of balance equations governing the shape of inextensible ribbons have been derived [12]. It was later shown that these equations can be mapped onto a rod theory provided an extra internal variable is added to enforce inextensibility [13]. Interestingly, triangular faceted ribbon has been found to be solution of the equations using numerical methods highlighting localized regions with high mean curvature [14]. More generally, faceted ribbons are examples of singular shape which have been studied extensively in the context of crumpled sheets [15] which are usually modeled as interacting elastic singularities forming a complex network of folds [16–23].

A second approach is based on a seminal work by Green [24, 25] who derived a set of equilibrium equations assuming that the ribbon has a small but finite thickness thus experiencing bending and stretching mode upon twisting. These equations can be obtained from the Föppl-von Kármán equations [26] and can be extended to a covariant version to capture finite rotations effect [27, 28]. The observed wrinkling and buckling instabilities can be quantitatively understood using a linear stability analysis[24, 26, 28]. Above threshold, it was shown experimentally that the wrinkling pattern continuously evolves into a triangular facets with singularities characterized by high mean and Gaussian curvatures.

While current models can capture some of the behaviors of a twisted ribbon, the crumpled phase is not fully understood either by the inextensible theory and by near threshold approach of thin extensible sheets. However, promising models allowing to incorporate extensibility effect in a developed post-buckling regime have been recently proposed, namely the Far from Threshold and the asymptotic isometry approaches [28–30]. The main finding of this paper is the identification of two regimes in the crumpled phase of a twisted ribbon depending on the applied tension. In a high-T regime, a Far from Threshold approach is found to capture quantitatively the experimental data. In a low-T regime, we propose to model the ribbon using the concept of asymptotic isometry.

The paper is organized as follows. We first describe the experimental set-up used to measure the contraction and torque response of twisted ribbon under constant load and describe briefly the phenomenology observed. We then model the ribbon as a thin extensible sheet to obtain the analytical expression of the contraction and torque in the uncrumpled, helicoidal regime. Next, we

analyze the crumpled phase using a Far from Threshold approach and the concept of asymptotic isometry. Finally, we summarize our findings and discuss some of their implications.

Experimental setup

In the present experiment, an initially flat ribbon is stretched by a constant load F and twisted by an angle θ using clamped boundary conditions (Fig. 1(a)). The ribbon is composed of cellulose acetate which has a linear elastic response for strains less than 2%. Young's modulus is $E \simeq 2.2\,\mathrm{GPa}$ and Poisson ratio $\nu = 0.35 \pm 0.05$. The thickness is $t = 256\,\mu\mathrm{m}$, width $W = 35\,\mathrm{mm}$ and length $L = 331\,\mathrm{mm}$. A torque sensor is placed at the lower clamp which can only rotate around the longitudinal axis and a load cell at the upper clamp whose vertical position can be adjusted through the end-to-end distance D between the two clamps. Non dimensional control parameters associated with tension and twist are :

$$T \equiv F/(EhW), \quad \eta \equiv \theta W/L, \tag{1}$$

respectively. We introduce the confinement parameter :

$$\alpha \equiv \eta^2/T \tag{2}$$

which can be interpreted as the ratio of geometrical over tensile strains. The torque is normalized by EW^2h. The contraction χ is measured using the relation $D = L(1-\chi)$. Because of the obvious contribution of the tension T, we introduce $\Delta\chi = \chi + T$ which is the contraction using the stretched untwisted configuration as reference (see notations in Fig. 1(b)). In practice, upon twisting the ribbon, the prescribed load F is kept constant by continuously adjusting D. Fig. 1(b) presents schematics of the ribbon morphology when increasing η continuously from zero starting from a pre-streched configuration at moderate T (Regime I). At small twist (Regime II) the shape is a stretched helicoid up to a threshold η_c above which longitudinal wrinkles are observed in the central part of the ribbon (Regime III) and expands laterally as the twist is increased. Very far from threshold (Regime IV), ordered crumpled, triangularly faceted ribbon is observed characterized localization of the curvature and plastic deformations near the long edges while the rest of the ribbon undergoes reversible deformations. The ribbon morphology has been described and characterized elsewhere in details [4]. Fig. 1(c) and (d) show the (Γ-η) and ($\Delta\chi$-η) curves respectively which are measured across the various morphological regimes mentioned above. When twisted up to an angle $\theta = 500\mathrm{deg}$ ($\eta \approx 1$, the ribbon shows a remarkable capacity to contract by almost 5%. Unlike the classical response of circular rod, we observed a strong nonlinear contraction of the ribbon $\Delta\chi$ and a nonlinear increase of the torque even for small twist. In this paper, we aim at explaining the nonlinear mechanical response of the ribbon near (Regimes I, II, and III) and very far (Regime IV) from threshold building on previous studies [4, 25, 26, 28].

Pre-buckling regime

To obtain the contraction and torque as a function of control parameters near threshold, we start by calculating the energy of a stretched helicoid ribbon loosely following [26]. The contraction χ and torque Γ can be formally expressed as :

$$\chi(\eta, T) = \left.\frac{\partial U}{\partial T}\right|_{\eta} \quad \text{and} \quad \Gamma(\eta, T) = \left.\frac{\partial U}{\partial \eta}\right|_{T} \tag{3}$$

where $U = U_s + U_b - W_T$ is the total energy of the system normalized by $EtWL$. $W_T = -\chi T$ is the work exerted by the load, the stretching energy U_s and bending energy U_b are given by [31]:

$$U_s = \frac{1}{2}\int dy \left[(\sigma_{xx}+\sigma_{yy})^2 - 2(1+\nu)\left(\sigma_{xx}\sigma_{yy} - \sigma_{xy}^2\right)\right] \tag{4}$$

and

$$U_b = \frac{1}{2}B\int dy \left[H^2 - 2(1-\nu)G\right], \tag{5}$$

respectively. σ_{ij} is the in-plane stress, H the mean curvature, G the Gaussian curvature, and $B = t^2/(12(1-\nu^2))$ the normalized bending stiffness. All stresses are normalized by Young's modulus and length by ribbon's width. x and y are the normalized longitudinal and transverse coordinates.

In the regime of small twist ($\theta \ll 1$), the ribbon's midplane can be parametrized by the deflection $w(x, y)$ in the z direction. The mean curvature is then given by $H \approx \frac{1}{2}\left(\frac{\partial^2 w}{\partial x^2} + \frac{\partial^2 w}{\partial x^2}\right)$ and the Gaussian curvature by $G \approx \frac{\partial^2 w}{\partial x^2}\frac{\partial^2 w}{\partial y^2} - \left(\frac{\partial^2 w}{\partial x \partial y}\right)^2$. In order to calculate the stresses and curvatures appearing in Eq. 4 and Eq. 5, we solve the Föppl-von Kármán equations given by [31]:

$$B\Delta^2 w = \frac{\partial^2\phi}{\partial x^2}\frac{\partial^2 w}{\partial y^2} + \frac{\partial^2\phi}{\partial y^2}\frac{\partial^2 w}{\partial x^2} - 2\frac{\partial^2\phi}{\partial x\partial y}\frac{\partial^2 w}{\partial x\partial y} \tag{6}$$

$$\Delta^2\phi = -\left[\frac{\partial^2 w}{\partial x^2}\frac{\partial^2 w}{\partial y^2} - \left(\frac{\partial^2 w}{\partial x\partial y}\right)^2\right] \tag{7}$$

where ϕ is Airy's potential which is related to the in-plane stress by $\sigma_{xx} = \frac{\partial^2\phi}{\partial y^2}$, $\sigma_{yy} = \frac{\partial^2\phi}{\partial x^2}$ and $\sigma_{xy} = -\frac{\partial^2\phi}{\partial x\partial y}$. The equations of equilibrium are complemented by the following boundary conditions :

$$\sigma_{yy}(y = \pm 1/2) = \sigma_{xy}(y = \pm 1/2) = 0, \tag{8}$$

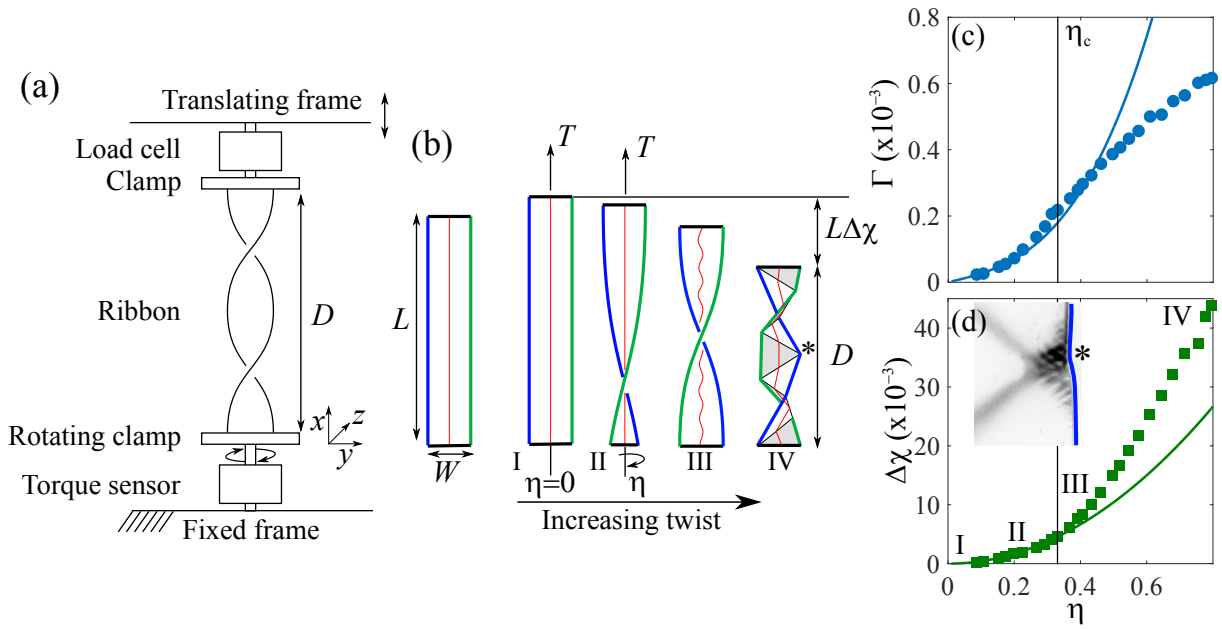

FIG. 1. (a) Sketch of the experimental setup. A ribbon is twisting by a normalized angle η under fixed tension T by means of a rotating clamp and adjustable end-to-end distance D. (b) Upon twisting, the ribbon goes from an initially stretched planar configuration (I) to a helicoid (II), a longitudinal buckled helicoid above a threshold η_c (see Eq. 16), and finally an ordered crumpled, triangularly faceted ribbon (IV) far from threshold. Below a threshold (red solid line), the nonlinear increase of the normalized torque Γ (c) and the corresponding normalized contraction $\Delta\chi$ (d) are in quantitative agreement with predictions given by Eq. 15 and Eq. 13(solid blue lines) without adjustable parameters. Here $T = 2.9 \times 10^{-3}$. Deviations from predictions are observed above threshold. At large η_c , Γ is found to increase linearly with η.

and the condition of vertical equilibrium :

$$T = \int_{-1/2}^{1/2} dy\, \sigma_{xx}. \tag{9}$$

We look for solution for Eqs. 6 and 7 assuming that the ribbon is a helicoid with a small twist angle yielding the following form for the deflection :

$$w(x, y) = \eta x y \tag{10}$$

We can readily check that $H = 0$ and $G = -\eta^2$ as expected for a helicoid. Further, we assume that the stress field is invariant along the x direction, thus, only depending on the y coordinate. This assumption greatly simplifies the calculation of the stress field since Eq. 7 now reads $\partial^4\phi/\partial y^4 = \eta^2$ and can be easily integrated to give:

$$\phi = \frac{1}{24}\eta^2 y^4 - \frac{1}{2}\chi y^2 \tag{11}$$

where we anticipated that the integration constant is the contraction χ. We omit x dependent terms because they would lead to non zero transverse and shear stresses at $y = \pm 1/2$ which are incompatible with the free boundary condition at the long edges (Eq. 8). The stress components are then given by :

$$\sigma_{yy} = \sigma_{xy} = 0, \quad \sigma_{xx} = -\chi + \frac{1}{2}\eta^2 y^2 \tag{12}$$

Inserting Eq. 12 into Eq. 9, the expression of the contraction reads:

$$\chi = \frac{1}{24}\eta^2 - T, \quad \Delta\chi = \eta^2/24 \tag{13}$$

It should be noted that the solutions obtained here, namely the stress field, the mean and Gaussian curvature, are still valid even for a finite twist angle θ provided $\eta \ll 1$ [28]. In our derivation, we only used Eq. 7 which is related to the in-plane force balance. One can easily check that the normal force balance given by Eq. 6 is trivially satisfies as well. Interestingly, the bending term in the r.h.s. of Eq. 6 which is proportional to $B\Delta H$ has no contribution provided the ribbon remains in a helicoid shape ($H = 0$).

Using Eq. 12 and Eq. 10, the total energy per unit length is therefore given by

$$U = \frac{1}{1440}\eta^4 + \frac{1}{24}T\eta^2 - \frac{1}{2}T^2 + 2B\eta^2 \tag{14}$$

The first three terms are associated with the contribution from the stretching energy and the work of the load while the last term is a bending terms proportional to t^2. The contraction and torque can now be calculated. The contraction is already known from Eq. 13 but one can check that the expression obtained is compatible with Eq. 3. Using Eq. 3, the torque is given by :

$$\Gamma = \frac{1}{12}\eta T + \frac{1}{360}\eta^3 + 4B\eta \tag{15}$$

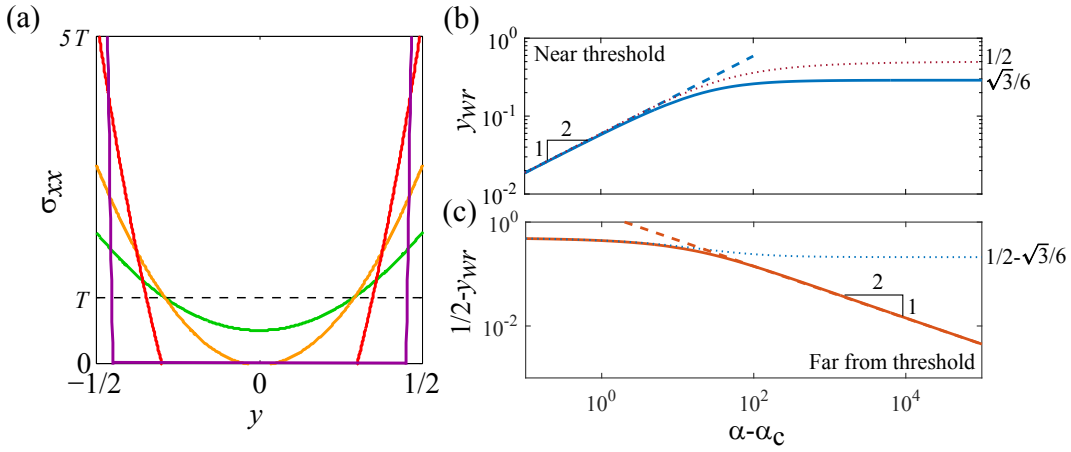

FIG. 2. (a) Longitudinal stress profile σ_{xx} as function of y for $\alpha = 12$, 24.5, 66, 700 and $B = 0$. A compressive zone of width $2y_{wr}$ develops for $\alpha > \alpha_c = 24$. Far from threshold $\alpha \gg \alpha_c$, the central compressive stress is set to zero while near the edge the profile remains parabolic (see Eq. 17). (b) The wrinkling zone half width y_{wr} scales as $(\alpha - \alpha_c)^{1/2}$ near threshold. (b) The width of the stretched band near the edge $1/2 - y_{wr}$ scales as $(\alpha - \alpha_c)^{-1/2}$ far from threshold. The curves in (b) and (c) are obtained by solving numerically Eq.18.

TABLE I. Scalings for the contraction $\Delta\chi$ and ΔK, the torque Γ and C, the wrinkle zone half width y_{wr} and the tensile flap width $1/2 - y_{wr}$ in the Near Threshold (NT) and Far from Threshold (FT) limit.

	$\Delta\chi = \chi + T$	$\Delta K = \Delta\chi/T$	Γ	$C = \Gamma/(\eta T)$	y_{wr}	$1/2 - y_{wr}$
NT ($\alpha \sim \alpha_c$)	$\frac{1}{24}\eta^2$	$\frac{1}{24}\alpha$	$\frac{1}{12}\eta T\left(1 + \frac{\alpha}{30}\right)$	$\frac{1}{12} + \frac{\alpha}{360}$	$\sim (\alpha - \alpha_c)^{1/2}$	$\sim \frac{1}{2}$
FT ($\alpha \gg \alpha_c$)	$\frac{1}{8}\eta^2$	$\frac{1}{8}\alpha$	$\frac{1}{4}\eta T$	$\frac{1}{4}$	$\sim \frac{1}{2}$	$\sim (\alpha - \alpha_c)^{-1/2}$

Eq. 15 extends the formula first derived by Green [25] where the effect of a small but finite tension is now included. Let us now evaluate the contribution of the bending and stretching energies. Although bending terms does not contribute to the normal force balance, they enter in the energy through the Gaussian curvature giving a term that scales as $U_b \sim t^2\eta^2$. The scaling for the stretching energy depends on the combination of T and η. At negligible twist ($\eta^2 \ll T$), $U_s \sim T^2 \gg t^2\eta^2 \sim U_b$, therefore the bending energy is negligible. At larger twist ($\eta^2 \sim T$), $U_s \sim \eta^2 T \sim \eta^4$. Bending energy can be neglected provided $T \gg t^2$. Except for very low tension, bending term can be safely neglected given the experimental parameters used. The case $\eta^2 \gg T$ corresponds to the post-buckling regime where the ribbon's shape is qualitatively different from a smooth helicoid and will be addressed in the next section.

In Fig. 1(c) and (d), we show that the measured torque and contraction are in the very good agreement with our predictions for small enough η without adjusting parameters. At larger η, longitudinal wrinkles develop leading to folds which are responsible for significant deviations from the predictions near threshold. In the following, we analyze the post-buckling behavior of the ribbon using a Far from Threshold approach.

High T crumpled regime

We propose to develop an understanding of the ribbon's behavior far from threshold when $\eta \gg \eta_c$ using an approach recently proposed in Ref. [29]. Here η_c (or equivalently α_c) is the twist angle threshold obtained from a linear stability analysis and is given by [4, 26]:

$$\eta_c = \sqrt{24T} + ct \tag{16}$$

where $c \sim 10$ depends slightly ν. Whereas a linear stability analysis is valid for configuration sufficiently close to threshold allowing to take the pre-buckling state as a reference configuration, a Far from Threshold approach is based on another ground because it assumes that the wrinkles strongly affects the stress field. More specifically, when $\alpha \gg \alpha_c$, the reference state is assumed to be a combination of tensile regions and wrinkled regions without compression. In the limit of vanishing thickness, wrinkles in the central part can adjust their shape to relax compression at no significant bending cost. To allow a quantitative analytical approach, the stress field of the ribbon is that of a stretched pre-buckled ribbon characterized by a parabolic profile except that inside the wrinkled zone ($|y| < y_{wr}$) the stress is zero (see Fig. 2). The proposed form for the longitudinal stress is therefore [28]

:

$$\sigma_{xx}^{FT} = \begin{cases} \frac{\eta^2}{2}(y^2 - y_{wr}^2), & \text{if } |y| < y_{wr} \\ 0, & \text{if } |y| > y_{wr} \end{cases} \quad (17)$$

where y_{wr} is set by the condition of vertical equilibrium, yielding :

$$1 - 12y_{wr}^2 + 16y_{wr}^3 = \frac{24}{\alpha} \quad (18)$$

As shown in Fig. 2, when $\alpha \gg \alpha_c$, y_{wr} tends to $1/2$ meaning that the wrinkling structure invades the entire width of the ribbon while the stretching part is confined to a flap near the edge of vanishing width. More precisely, the width of the stretching flap is given by $1/2 - y_{wr} \approx \sqrt{\frac{2}{\alpha}}$. We can readily check that the stress field proposed here satisfies the boundary conditions and the equation of in-plane equilibrium. The contraction is now given by :

$$\chi = \frac{\eta^2}{2} y_{wr}^2 \quad (19)$$

generalizing the expression given in Eq. 13.

We will now calculate the energy of the ribbon far from threshold, in the asymptotic limit $\alpha \gg \alpha_c$. When calculating the total energy of the ribbon, the stretching is found to scale as α^{-1}, the work of load which scales as α is therefore dominating. In the Far from Threshold limit, the total energy of the ribbon reduces to the work of the load and is given by :

$$U_\infty^{FT} \approx -W_T = \frac{1}{8}\eta^2 T \quad (20)$$

Using Eq. 13 and 15, we obtain:

$$\chi_\infty^{FT} = \frac{1}{8}\eta^2, \quad \Gamma_\infty^{FT} = \frac{1}{4}\eta T. \quad (21)$$

It will be convenient to define a normalized contraction $\Delta K = \Delta\chi/T$ and torque $C = \Gamma/(\eta T)$ yielding:

$$\Delta K_\infty^{FT} = \frac{\alpha}{8}, \quad C_\infty^{FT} = \frac{1}{4} \quad (22)$$

All the scalings obtained are summarized in Table I.

Comparing these predictions with our data, the contraction is quantitatively captured by our analysis. We identify a transition from near to far from threshold for $\alpha \sim 10^2$ which is observed to be T independent. The corresponding measured torque reveals however a more complex trend. For $\alpha > 10^2$, the torque deviates from the near threshold prediction but the trend is observed to depend on the applied tension unlike the contraction response. More precisely, the torque is found to globally decrease with T and exhibits a weak dependence on α which can be captured by a scaling of the form $C \sim \alpha^p$ with a small exponent p. The scaling $C \sim \alpha^{1/6}$ is shown as a guide for the eyes. In a first approximation, this dependence is however neglected, thus, we assume that a plateau, denoted C_∞^{FT}, is reached at large α. As shown in Fig. 4, C_∞^{FT} decreases with T and reaches asymptotically the value $1/4$ which is precisely the prediction given in Eq. 21. We conclude that a Far from Threshold analysis can quantitatively explain the contraction and torque response of a twisted ribbon in a crumpled phase for sufficiently high tension. In this high-T crumpled regime, stretching energy most likely dominates bending energy, thus, the Far from Threshold approach which neglects the bending contribution of the folds in the stress field provides accurate predictions. However, at smaller tension, the stress field may be qualitatively different from the proposed form given Eq. 17 indicating that the large curvatures along ridges and vertices now contribute significantly to the stress. The change of regime is further substantiated when measuring the aspect ratio λ/W of the triangular facets formed by to two successive fold. We do not oberve a significant influence of the twist on the triangle shape. However, when decreasing the tension, we found a transition at $T > 1 \times 10^{-2}$ where the aspect ratio sharply increases until reaching a plateau $\lambda/W \approx 2$. No higher value of λ/W could be obtained by reducing further the tension.

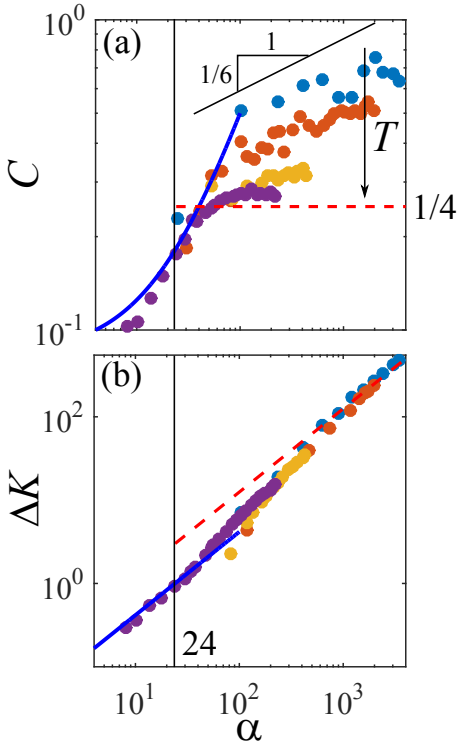

FIG. 3. Evolution of $C = \Gamma/(\eta T)$ and $K = \chi/T$ as a function of α for $T = 0.2\times10^{-3}$, 0.4×10^{-3}, 1.6×10^{-3}, 2.9×10^{-3}. The blue lines correspond to the pre-buckling predictions. The red dashed line correspond to the Far from Threshold approach predictions given by Eqs. 22 and 20

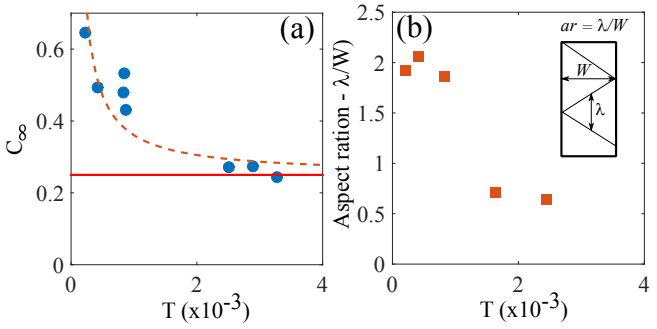

FIG. 4. Evolution of the asymptotic value of C_∞ for $\alpha \gg 24$. At large T, C tends to the value 1/4, predicted by the far from threshold approach. This large T regime corresponds to small triangular facets.

Low T crumpled regime

In order to understand the crumpled state at low tension, we introduce a specific form for the energy recently suggested to model a regime of asymptotic isometry where both the thickness and the tension tend to zero :

$$U^{Cr} = U_\infty^{FT} + \frac{1}{2n}\gamma B \eta^{2n}, \tag{23}$$

where γ is a numerical prefactor and n an adjustable exponent. The first term correspond to the contribution of the stretching energy in the Far from Threshold limit. The second term captures the contribution of the bending energy originating the focusing the curvature near the triangular tips. The value of n can be inferred by inspection of the experimental data. For $n \neq 1$, C would have a significant dependence with η which is not observed in our data, therefore we found that our data are best rationalized taking $n = 1$ leading to :

$$C_\infty^{Cr} = \frac{1}{4} + \gamma \frac{B}{T}. \tag{24}$$

We can also note that the good agreement of the FT approach to model the contraction, even at large α, indicates that the extra bending terms added in Eq. 23 does not depend on the tension leaving the scaling for χ unaffected. Taking $\gamma \approx 20$, data shown in Fig. 4 are well adjusted by Eq. 24.

Conclusions

In conclusion, we characterized experimentally and modeled the torque and contractile response of a twisted ribbon in a crumpled state. The pre-crumpled state is quantitatively captured when solving the FvK equations. At large twist angle, the ribbon exhibits a crumpled state which cannot be capture from inextensible thin sheet theories. We identified two regimes depending on the tension. In a high-T crumpled regime, the macroscopic response is dominated by the external work of the load which can be quantitatively capture by a Far from Threshold approach which neglects the contribution of the folds. In a low-T crumpled regime, bending contributions originating from the localized curvatures strongly affect the torsional response but not the contraction. This behavior at low tension can be understood introducing the concept of asymptotic isometry where both stretching and localized bending are taken into account. More work is needed to connect global behavior with the local response as the proposed models for the crumpled states are still partially phenomenological.

Acknowledgments

We thank Kévin Flijane and Gaëtan Gourgaud for their help with the experiment and Vincent Demery and Arshad Kudrolli for stimulating discussions. This work was funding by Ciência Sem Fronteiras program (CNPq, Brazil) 313029/2013-05.

* julien.chopin@espci.fr

[1] S. Xu, Y. Zhang, J. Cho, J. Lee, X. Huang, L. Jia, J. A. Fan, Y. Su, J. Su, H. Zhang, *et al.*, Nature communications **4**, 1543 (2013).
[2] M. D. Lima, S. L. Fang, X. Lepro, C. Lewis, R. Ovalle-Robles, J. Carretero-Gonzalez, E. Castillo-Martinez, M. E. Kozlov, J. Y. Oh, N. Rawat, C. S. Haines, M. H. Haque, V. Aare, S. Stoughton, A. A. Zakhidov, and R. H. Baughman, Science **331**, 51 (2011).
[3] O. O. Kit, T. Tallinen, L. Mahadevan, J. Timonen, and P. Koskinen, Physical Review B **85**, 085428 (2012).
[4] J. Chopin and A. Kudrolli, Phys. Rev. Lett. **111**, 174302 (2013).
[5] J. Chopin and A. Kudrolli, http://arxiv.org/abs/1601.00575 (2016).
[6] J. Chopin, D. Vella, and A. Boudaoud, Proceedings of the Royal Society A-mathematical Physical and Engineering Sciences **464**, 2887 (2008).
[7] H. King, R. D. Schroll, B. Davidovitch, and N. Menon, Proc. Natl. Acad. of Sci. U.S.A. **109**, 9716 (2012).
[8] H. Aharoni and E. Sharon, Nat. Mater. **9**, 993 (2010).
[9] B. Audoly and Y. Pomeau, *Elasticity and geometry*, edited by O. Press (2010).
[10] M. Sadowsky, Preuss. Akad. Wiss. **22**, 412 (1930).
[11] W. Wunderlich, Monatshefte für Mathematik **66**, 276 (1962).
[12] E. Starostin and G. Van Der Heijden, Nature materials **6**, 563 (2007).
[13] M. A. Dias and B. Audoly, J. Elast. **119**, 49 (2015).
[14] A. P. Korte, E. L. Starostin, and G. H. M. van der Heijden, Proc. R. Soc. A **467**, 285 (2011).

[15] T. A. Witten, Rev. Mod. Phys. **79**, 643 (2007).
[16] A. Lobkosvky, S. Gentges, H. Li, D. Morse, and T. A. Witten, Science **270**, 1482 (1995).
[17] M. Ben Amar and Y. Pomeau, Proc. R. Soc. A **453**, 729 (1997).
[18] E. Cerda, S. Chaieb, F. Melo, and L. Mahadevan, Nature **401**, 46 (1999).
[19] S. Chaieb, F. Melo, and J. C. Geminard, Phys. Rev. Lett. **80**, 2354 (1998).
[20] A. Boudaoud, P. Patricio, Y. Couder, and M. Ben Amar, Nature **407**, 718 (2000).
[21] D. L. Blair and A. Kudrolli, Phys. Rev. Lett. **94**, 166107 (2005).
[22] T. Tallinen, J. A. Astrom, and J. Timonen, Nature Materials **8**, 25 (2009).
[23] J. Guven, J. Hanna, O. Kahraman, and M. M. Muller, Eur. Phys. J. E **36**, 1 (2013).
[24] A. Green, Proceedings of the Royal Society of London. Series A, Mathematical and Physical Sciences **154**, 430 (1936).
[25] A. E. Green, Proc. R. Soc. A **161**, 197 (1937).
[26] C. D. Coman and A. P. Bassom, Acta Mech. **200**, 59 (2008).
[27] E. M. Mockensturm, J. Appl. Mech. **68**, 561 (2001).
[28] J. Chopin, V. Demery, and B. Davidovitch, J. Elast. **119**, 137 (2015).
[29] B. Davidovitch, R. D. Schroll, D. Vella, M. Adda-Bedia, and E. A. Cerda, Proc. Natl. Acad. of Sci. U.S.A. **108**, 18227 (2011).
[30] D. Vella, J. S. Huang, N. Menon, T. P. Russell, and B. Davidovitch, Physical Review Letters **114**, 014301 (2015).
[31] L. D. Landau and E. Lifshitz, Course of Theoretical Physics **3**, 109 (1986).